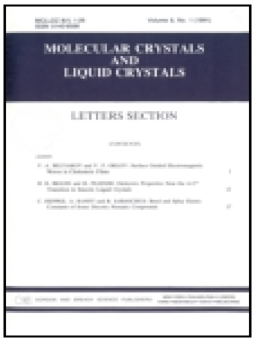
MOLECULAR CRYSTALS AND LIQUID CRYSTALS

LETTERS SECTION

Molecular Crystals and Liquid Crystals

ISSN: 1542-1406 (Print) 1563-5287 (Online) Journal homepage: http://www.tandfonline.com/loi/gmcl20

Efficiency Improvement of Dye-sensitized Solar Cells by Phosphor (Y_2O_3:Er^{3+}, $Y_3Al_5O_{12}$:Ce^{3+}) Co-doped TiO_2 Electrodes

Young Moon Kim, Chang Seob Kim & Hyung Wook Choi

To cite this article: Young Moon Kim, Chang Seob Kim & Hyung Wook Choi (2015) Efficiency Improvement of Dye-sensitized Solar Cells by Phosphor (Y_2O_3:Er^{3+}, $Y_3Al_5O_{12}$:Ce^{3+}) Co-doped TiO_2 Electrodes, Molecular Crystals and Liquid Crystals, 620:1, 83-90, DOI: 10.1080/15421406.2015.1094874

To link to this article: http://dx.doi.org/10.1080/15421406.2015.1094874

Mol. Cryst. Liq. Cryst., Vol. 620: pp. 83–90, 2015
Copyright © Taylor & Francis Group, LLC
ISSN: 1542-1406 print/1563-5287 online
DOI: 10.1080/15421406.2015.1094874

Efficiency Improvement of Dye-sensitized Solar Cells by Phosphor (Y_2O_3:Er^{3+}, $Y_3Al_5O_{12}$:Ce^{3+}) Co-doped TiO_2 Electrodes

YOUNG MOON KIM,[1] CHANG SEOB KIM,[2]
AND HYUNG WOOK CHOI[1,*]

[1]Department of Electrical Engineering, Gachon University, Sujeong-Gu, Seongnam-Si, Gyeonggi-Do, Korea
[2]Department of Energy IT, Gachon University, Sujeong-Gu, Seongnam-Si, Gyeonggi-Do, Korea

Generally, the (N-719) dye used in dye-sensitized solar cells (DSSCs) only absorbs visible light in the wavelength range from 400 to 700 nm. Most of the ultraviolet and infrared rays from the sun are not utilized by this dye. However, ultraviolet and infrared rays can be converted to visible light by upconversion luminescence. Such visible light can then be reabsorbed by the dye, allowing for a greater range of solar irradiation to be utilized in DSSCs. A mixed phosphor of $Y_3Al_5O_{12}$:Ce^{3+} *and* Y_2O_3:Er^{3+}*, acting as luminescence medium, was added to the* TiO_2 *electrode of DSSCs, increasing the photocurrent density and efficiency as a result of the upconversion. The* $Y_3Al_5O_{12}$:Ce^{3+}/Y_2O_3:Er^{3+} *phosphor-co-doped* TiO_2 *electrode cells showed better performance than the phosphor-free cells. In this paper, we describe the characterization of DSSCs containing the mixed* $Y_3Al_5O_{12}$:Ce^{3+}/Y_2O_3:Er^{3+} *phosphor and discuss the enhanced efficiencies of the DSSCs as compared with those of phosphor-free cells.*

Keywords DSSCs; TiO_2; Phosphor; Phosphor-mixed DSSC

Introduction

Since they were first introduced by Gratzel and O'Regan in 1991, considerable effort has been devoted to the study of dye-sensitized solar cells (DSSCs) [1]. As promising next-generation alternatives to solid-state photovoltaic devices, DSSCs have attracted attention because of their low production costs, environmentally friendly components, and relatively high conversion efficiencies [2–3]. Moreover, enhancing DSSC efficiency would provide enormous economic advantages [4–8]. Although DSSC development has progressed significantly over the past decade [9–11], enhancing DSSC efficiency and reducing production costs are still crucial challenges. One approach to increasing the efficiencies of DSSCs is to enhance their ability to harvest light [12–13]. Many dyes have been synthesized and employed in the interest of improving the photocurrent production of DSSCs. Currently, one

---

[*]Address correspondence to Prof. Hyung Wook Choi, Department of Electrical Engineering, Gachon University, 1342 SeongnamDaero, Sujeong-gu, SeongNam-si, Gyeonggi-do 461-701, Korea (ROK). E-mail: chw@gachon.ac.kr

Color versions of one or more of the figures in the article can be found online at www.tandfonline.com/gmcl.

of the most reliable, commercially available dyes is N-719, which has long been considered the standard for many DSSC systems [14–16]. However, N-719 only absorbs visible light in the wavelength range from 400 to 700 nm, and therefore does not allow for the utilization of most infrared and ultraviolet solar radiation [9]. If infrared and ultraviolet radiation could be converted to visible light by conversion luminescence and then reabsorbed by the DSSC dye, a larger range of solar radiation could be utilized, effectively enhancing the DSSC photocurrent. Employing phosphors in DSSCs is known to be an effective method for improving their ability to harvest incident light [12–13]. With this in mind, we produced DSSCs with mixed $Y_3Al_5O_{12}$:Ce^{3+}/Y_2O_3:Er^{3+} phosphor-co-doped TiO_2 electrodes. In this paper, we describe the characterization of DSSCs containing mixed $Y_3Al_5O_{12}$:Ce^{3+}/Y_2O_3:Er^{3+} phosphors with varying ratios of $Y_3Al_5O_{12}$:Ce^{3+} and Y_2O_3:Er^{3+} and discuss their enhanced efficiencies as compared with those of phosphor-free cells.

Experimental

The $Y_3Al_5O_{12}$:Ce^{3+} phosphor was prepared by the combustion method. The starting materials for fabricating the YAG:Ce phosphor were $Y(NO_3)_3{\cdot}6H_2O$(99.9%, Aldrich), $Al(NO_3)_3{\cdot}9H_2O$ (99.997%, Aldrich), and $Ce(NO_3)_3{\cdot}6H_2O$ (99.999%, Aldrich). Urea was used as a reagent. $Y(NO_3)_3$, $Al(NO_3)_3$, and $Ce(NO_3)_3$ solutions were dissolved in deionized water. The solution was then stirred with a magnetic bar on a hot plate for 30 min in air. The mole ratio of all metal ions to urea was maintained at 1:1. The solution was heated to 100°C and stirred until the mixture became transparent. Next, the solution was rapidly heated to 300°C for combustion, which turned the solution bright yellow. After a few minutes, the solution underwent combustion, releasing a brown gas. The combustion process yielded the precursor, which was dried in air and sintered at 1000°C for 2 h in an alumina crucible in a box furnace.

The Y_2O_3:Er^{3+} phosphor was prepared using a urea homogeneous precipitation method. The starting materials were yttrium(III) oxide (Y_2O_3, 99.99%, Aldrich), erbium(III) oxide (Er_2O_3, 99.99%, Aldrich), nitric acid (A.C.S. reagent, 70%), and urea (NH_2CONH_2, Aldrich). Y_2O_3:Er^{3+} powders with compositions of $(Y_{1-x}Er_x)_2O_3$ ($x = 0.03$) were prepared. The starting solutions were prepared by dissolving appropriate amounts of Y_2O_3 and Er_2O_3 in nitric acid. The total combined concentration of Er^{3+} and Y^{3+} was maintained at 0.015 M, and the concentration ratio of urea to metal ions was maintained at 35:1. The solution was stirred with a magnetic stirrer bar on a hot plate under aerobic conditions for 1 h in order to increase homogenization. The solution was then heated to 90°C and stirred for 6 h until a pH value of 7.5 was reached. Finally, the solution was allowed to cool to room temperature and the precipitate was separated using a membrane filter, washed with distilled water and ethanol, and dried in an oven at 60°C (in air) for 24 h. Portions of the powder were then sintered at 800°C for 2 h in an alumina crucible in a box furnace.

Titanium(IV) isopropoxide (TTIP, Sigma Aldrich), ethyl alcohol, nitric acid, and deionized water were used as the precursors for the TiO_2 particles. Mixed-phosphor(7.00 wt.%) TiO_2 pastes were prepared using the sol–gel method. Mixed-phosphor TiO_2 films were prepared by coating the pastes onto an FTO plate using the doctor blade technique (thickness : 15 μm). The mixed-phosphor TiO_2 cells were immersed in the N-719 dye solution for 24 h at room temperature. A counter electrode was prepared by spin coating a H_2PtCl_6 solution onto FTO glass and then heating the glass at 450°C for 30 min. The TiO_2 electrode with the adsorbed dye and the Pt counter electrode were assembled into a sandwich-type cell;

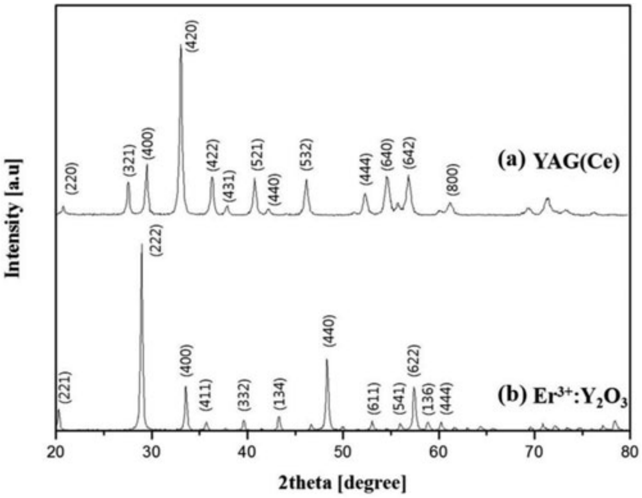

Figure 1. XRD patterns of the (a) $Y_3Al_5O_{12}:Ce^{3+}$ and (b) $Y_2O_3:Er^{3+}$ phosphors.

the assembly was then sealed with a 60-μm-thick hot-melt sealant. An electrolyte solution (iodide/tri-iodide, AN-50, Solaronix) was introduced through a hole drilled in the counter electrode and the hole was sealed with a cover glass. The morphology of the prepared phosphors was investigated using field-emission scanning electron microscopy (FE-SEM, model S-4700, Hitachi). The photoluminescence spectra were obtained using an FP-6200 spectrofluorometer with a 150 W Xe lamp (Jasco). The active area of the resulting cell exposed to light was approximately 0.25 cm^2 (0.5 cm × 0.5 cm). The absorption spectra of the electrode films were measured using an ultraviolet–visible (UV–vis) spectrometer (UV-vis 8453, Agilent). The conversion efficiency of the fabricated DSSCs was measured using an *I–V* solar simulator (Solar Simulator, McScience).

Results and Discussion

The structural characterization of the phosphor powders was performed by X-ray diffraction (XRD). The XRD pattern of the $Y_3Al_5O_{12}:Ce^{3+}$ phosphor at 1000°C is shown in Fig. 1(a). The main peak, YAG(420), appeared at the sintering temperature of 1000°C. Also, the YAG phase crystallized at 1000°C, which is in agreement with the Joint Committee on Powder Diffraction Standards (JCPDS) diffraction file 33-0040. The XRD pattern of the $Y_2O_3:Er^{3+}$ phosphor powder calcined at 800°C for 2 h is shown in Fig. 1(b). The XRD data obtained for the treated nanocrystalline materials show that only the cubic phase of Y_2O_3 was present; no other impurity peaks were observed.

The emission spectrum of the YAG:Ce phosphor powder sintered at 1000°C is shown in Fig. 2(a). The phosphor powder shows a broad emission peak over the range from 500 to 560 nm. As a result, the powder sample showed an emission band at 527 nm under excitation at 460 nm. The emission spectrum of the $Y_2O_3:Er^{3+}$ phosphor powder calcined at 800°C is shown in Fig. 2(b). The spectrum was obtained by monitoring the excitation at 980 nm. Two main emission bands were observed, one corresponding to green emission, centered at 560 nm, and one corresponding to red emission, centered at 660 nm. For the solution with a total metal ion concentration of 0.015 M, the spectrum consisted of two main emission bands, located at the same energies: the red emission, centered at 660 nm, and the green

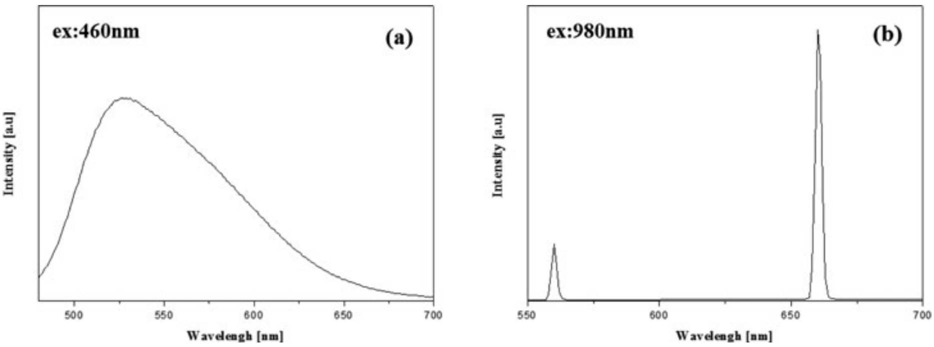

Figure 2. Emission spectra of (a) $Y_3Al_5O_{12}$:Ce^{3+} prepared at 1000°C and (b) Y_2O_3:Er^{3+} prepared at 800°C.

emission, centered at 560 nm, which correspond to the $^4F_{9/2}$–$^4I_{15/2}$ and $^4S_{3/2}$/$^2H_{11/2}$–$^4I_{15/2}$ Er3+ transitions, respectively.

Fig. 3(a) shows SEM images of the $Y_3Al_5O_{12}$:Ce^{3+} phosphor calcined at 1000°C. Uniform and spherical nanoparticles with homogeneous structures were obtained by the combustion method at 1000°C. The mean size of the particles measured using the SEM image was $<$50 nm. The morphology of the Y_2O_3:Er^{3+} phosphor powder calcined at 800°C is shown in Fig. 3(b). The mean size of the particles measured from the SEM image was

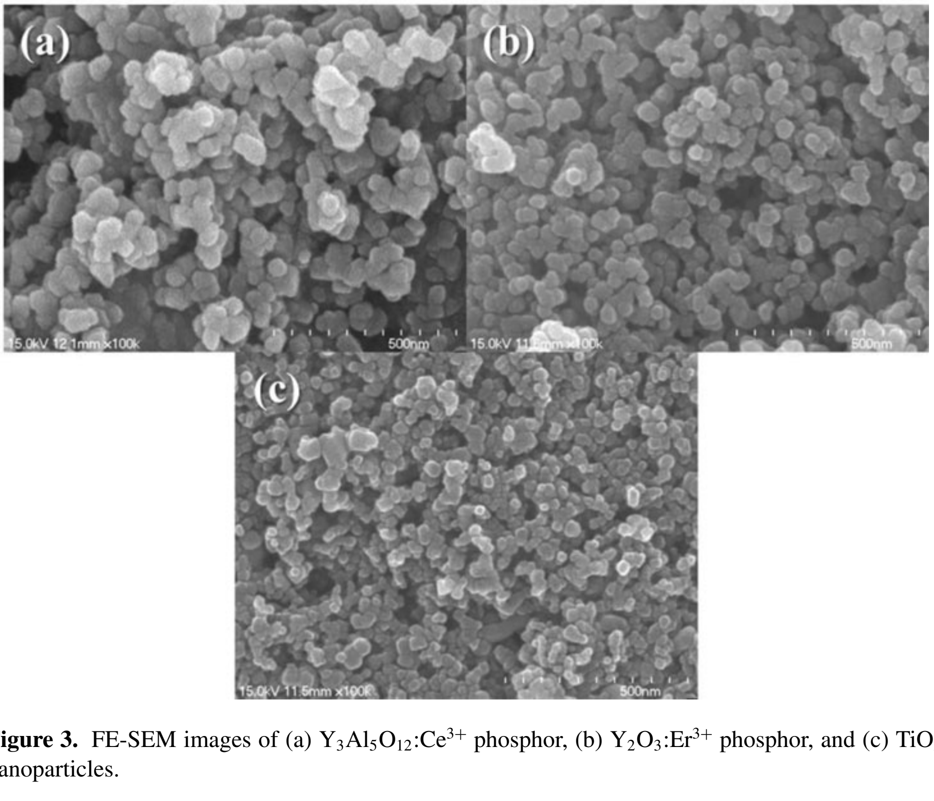

Figure 3. FE-SEM images of (a) $Y_3Al_5O_{12}$:Ce^{3+} phosphor, (b) Y_2O_3:Er^{3+} phosphor, and (c) TiO_2 nanoparticles.

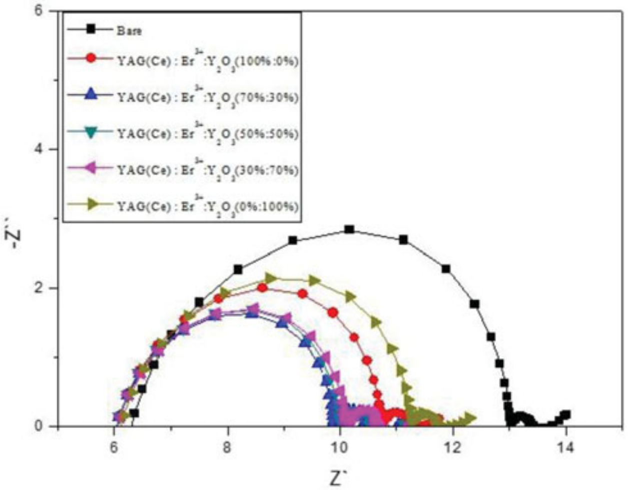

Figure 4. Nyquist plot of mixed-phosphor DSSC at open-circuit voltage.

50 nm. The TiO_2 nanoparticles prepared by the sol–gel method are shown in Fig. 3(c). The particles had a consistent diameter of 20–30 nm.

The Nyquist plots of DSSCs with five types of mixed phosphors at open-circuit voltage are shown in Fig. 4. Electrochemical impedance spectroscopy (EIS) is a useful method for analyzing charge-transport processes and internal resistances [17]. The R_{CT} values decreased the most at 7 and 3 wt% $Y_3Al_5O_{12}:Ce^{3+}:Y_2O_3:Er^{3+}$. At 7 and 3 wt%, the samples showed the highest absorbance over the wavelength range from 400 to 800 nm. The mixed-phosphor DSSCs produced higher short-circuit current density (J_{SC}) values, resulting in decreased R_{CT} values. However, the R_{CT} values increased when a $Y_2O_3:Er^{3+}$ phosphor ratio of more than 50% was used.

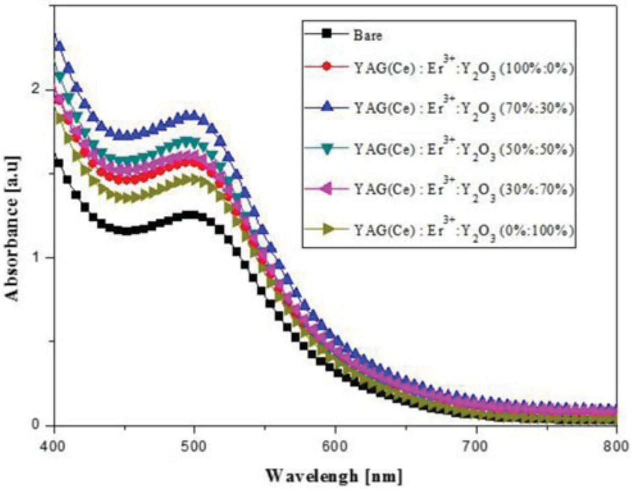

Figure 5. UV–vis absorbance of mixed-phosphor DSSCs.

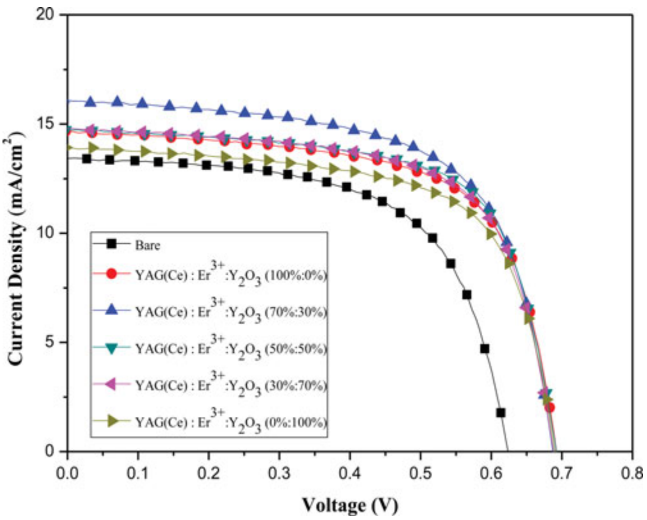

Figure 6. Photovoltaic parameters of DSSCs.

The UV–vis absorbance of the mixed-phosphor DSSCs is shown in Fig. 5. The N-719 dye only absorbs visible light in the wavelength range from 400 to 800 nm. However, the sample doped with the mixture containing 7 and 3 wt% $Y_3Al_5O_{12}:Ce^{3+}:Y_2O_3:Er^{3+}$ showed the highest absorbance over the wavelength range from 400 to 800 nm. Obviously, this was due to the conversion luminescence of the phosphor from reabsorption by the dye in the DSSC. Evidently, effective conversion luminescence of the phosphor via the mixed-phosphor TiO_2 electrode occurred.

The current–voltage photovoltaic performance curves of the phosphor-free DSSC and mixed-phosphor DSSCs under AM 1.5 illumination (100 mW/cm^2) are shown in Fig. 6. The equivalent values based on the weight ratios of the $Y_3Al_5O_{12}:Ce^{3+}$ and $Y_2O_3:Er^{3+}$ phosphors are summarized in Table 1. When the amount of the mixture added contained

Table 1. J_{SC}, V_{OC}, FF, and efficiency

Sample	V_{OC} (V)	J_{SC} (mA/cm^2)	FF (%)	Efficiency (η)
Bare	0.62	13.43	61.69	5.17
$Y_3Al_5O_{12}:Ce^{3+}:Y_2O_3:Er^{3+}$ (100%:0%)	0.69	14.66	65.21	6.62
$Y_3Al_5O_{12}:Ce^{3+}:Y_2O_3:Er^{3+}$ (70%:30%)	0.68	16.09	63.35	7.00
$Y_3Al_5O_{12}:Ce^{3+}:Y_2O_3:Er^{3+}$ (50%:50%)	0.69	14.72	66.91	6.82
$Y_3Al_5O_{12}:Ce^{3+}:Y_2O_3:Er^{3+}$ (30%:70%)	0.68	14.80	65.68	6.69
$Y_3Al_5O_{12}:Ce^{3+}:Y_2O_3:Er^{3+}$ (0%:100%)	0.69	13.91	64.95	6.24

7 and 3 wt% $Y_3Al_5O_{12}$:Ce^{3+}:Y_2O_3:Er^{3+}, the light-to-electric energy conversion efficiency of the DSSC reached 7%. The conversion efficiency was thus increased by a factor of 1.35 as compared to DSSCs without phosphor. The increase in J_{SC} is mainly due to the conversion luminescence of phosphor, which facilitates the harvesting of additional incident light [18]. However, the efficiency decreased when the ratio of Y_2O_3:Er^{3+} to $Y_3Al_5O_{12}$:Ce^{3+} was more than 50%. In particular, the N-719 dye absorbs light in the wavelength range from 400 to 600 nm, and the emission band of $Y_3Al_5O_{12}$:Ce^{3+} is the most intense at 500–600 nm. The results indicate that the J_{SC} values gradually decreased as the $Y_3Al_5O_{12}$:Ce^{3+} phosphor ratio decreased. The emission of Y_2O_3:Er^{3+} was relatively low as compared to that of $Y_3Al_5O_{12}$:Ce^{3+} at 400–600 nm. Consequently, the $Y_3Al_5O_{12}$:Ce^{3+} mixed-phosphor TiO_2 electrode showed better performance than did the Y_2O_3:Er^{3+} mixed-phosphor TiO_2 electrode. Further, the optimum condition for high conversion efficiency was the addition of a mixture containing 7 and 3 ($Y_3Al_5O_{12}$:Ce^{3+} : Y-$_2O_3$:Er^{3+}) wt%. The DSSC co-doped with a mixture containing 7 and 3 wt% exhibited a higher photocurrent density than did the bare cell because of the additional light harvesting by the mixed phosphor in the DSSCs.

Conclusions

The photovoltaic performance of DSSCs containing the mixed phosphors $Y_3Al_5O_{12}$:Ce^{3+} and Y_2O_3:Er^{3+} was compared. The UV radiation and infrared rays could be converted to visible light by conversion luminescence and then reabsorbed by the dye in the DSSCs, so that more solar irradiation could be utilized. Therefore, the use of $Y_3Al_5O_{12}$:Ce^{3+} and Y_2O_3:Er^{3+} should improve light harvesting and the photocurrent by conversion luminescence. When the mixed phosphor contained 7 and 3 ($Y_3Al_5O_{12}$:Ce^{3+}:Y_2O_3:Er^{3+}) wt%, the light-to-electric energy conversion efficiency of the DSSC reached 7% and increased by a factor of 1.35 as compared with that of the DSSC without phosphor. Therefore, increasing the amount of the light absorbed by DSSCs by using a phosphor may be an effective method of enhancing their efficiency.

Acknowledgments

This work was supported by the Human Resources Development program (No.20124030200010) of the Korea Institute of Energy Technology Evaluation and Planning(KETEP) grant funded by the Korea government Ministry of Trade, Industry and Energy. This work was supported by the National Research Foundation of Korea (NRF) Grant Funded by the Korean Government (MEST) (No. 2012R1A1A2044472).

References

[1] Suzuki, R., O'Regan, B., & Gratzel, M. (1991). *Nature 353*, 737.
[2] Heimer, T., Heilweil, E., Bignozzi, C., & Meyer, G. (2000). *J. Phys. Chem. A 104*, 4256.
[3] Yang, Y., Zhou, C., Xu, S., Hu, H., Chen, B., Zhang, J., Wu, S., Liu, W., & Zhao, X. (2008). *J. Power Sources 185*, 1492.
[4] Chappel, S., Chen, S. G., & Zaban, A. (2002). *Langmuir 18*, 3336.
[5] Bedja, I., Kamat, P. V., Hua, X., Lappin, A. G., Hotchandani, & S. (1997). *Langmuir 13*, 2398.
[6] Keis, K., Bauer, C., Boschloo, G., Hagfeldt, A., Westermark, K., Rensmo, H., & Siegbahn, H. (2002). *J. Photochem. Photobiol. Chem. 148*, 57.
[7] Chappel, S., & Zaban, A. (2002). *Solar Energy Mater Solar Cells 71*, 141.
[8] Guo, P., & Aegerter, M. A. (1999). *Thin Solid Films 351*, 290.

[9] Gratzel, M. (2001). *Nature 414*, 338.

[10] Gratzel, M. (2009). *Acc. Chem. Res. 42*, 1788.

[11] Hagfeldt, A., Boschloo, G., Sun, L., Kloo, L., & Pettersson, H. (2010). *Chem. Rev. 110*, 6595.

[12] Oelhafen, & P., Schuler, A., *Solar Energy 79* (2005) 110.

[13] Wang, Y., Chen, E., Lai, H., Lu, B., Hu, Z., Qin, X., Shi, W., & Du, G. (2013) *Ceram. Int. 39*, 5407.

[14] Wang, G., Lin, R., Lin, Y., Li, X., Zhou, X., & Xiao, X. (2005). *Eletrochim. Acta. 50*, 5546.

[15] Seo, H., Son, M.-K., Shin, I., & Kim, J.-K., Lee, K.-J., Prabakar, K., Kim, H.-J. (2010). *Electrochim. Acta*, *55*, 4120.

[16] Ryan, M. (2009). *Platinum Met. Rev.*, *53*, 216.

[17] Hsu, C. P., Lee, K. M., Huang, J. T. W., Lin, C. Y., Lee, C. H., Wang, L. P., Tsai, S. Y., & Ho, K. C. (2008). *Electrochim. Acta 53*, 7514.

[18] Chou, C. S., Guo, M. G., Liu, K. H., & Chen, Y. S. (2012). *Applied Energy*, Volume *92*, 224.